Tunneling through a Coherent "Quantum Antidot Molecule"

I. J. Maasilta* and V. J. Goldman
Department of Physics, State University of New York, Stony Brook, New York 11794-3800
(Received 27 July 1999)

We report experiments on resonant tunneling through a quantum antidot in the fractional quantum Hall regime. The envelope of the conductance peaks indicates tunneling via *two* resonant states, one of them bound on the lithographic antidot, the other on a hill of the disorder potential. Moreover, our analysis indicates that the coherent tunneling rate between the two states is an order of magnitude higher than the phase breaking rate, thus giving evidence for a coherently coupled "antidot molecule."

PACS numbers: 73.40.Gk, 73.40.Hm

In the quest for miniaturization of electronic devices a length scale has already been reached, where quantum mechanics dominates the behavior of electrons in semiconductors. A typical representative of such a device is a quantum dot, where electrons occupy discrete zero-dimensional (0D) quantum states [1,2]. The first steps towards building circuits with quantum dots utilizing *classical* logic (Coulomb blockade regime) have already been taken [3]. On the other hand, even more exciting is the prospect of taking full advantage of the quantum behavior by constructing *quantum* logic [4], which has been shown to be able to stretch the boundaries of practically computable problems [5]. If these quantum circuits are to be realized with elements like quantum dots [6], it is necessary to couple them coherently. This is a difficult task in the preferred planar geometry [7] due to problems in creating a thin enough barrier between the two dots [8]. Also, the role of electron-electron interactions is crucial at the lowest temperatures [9].

Considering the above mentioned difficulties we have studied the coherent coupling between two 0D quantum states in the quantum Hall (QH) regime. In the QH regime, the tunneling barriers are formed by the QH gap, which is easily orders of magnitude smaller than a typical electrostatic barrier, therefore allowing a large coupling with a much larger tunneling distance. The 0D states are formed around potential hills that are void of electrons. Here, one of the states is localized on a lithographically defined potential, a quantum antidot [10], whereas the other, we argue, is produced by the disorder potential. Additionally, in the fractional QH regime these states are not pure electron states, but fractionally charged Laughlin quasiparticles [11], whose effective interaction is reduced further compared to electron-electron interaction by virtue of the smaller value of the charge. Also, since we are adding charge to the edge of an open electron system, Coulomb blockade can be neglected. For these reasons, we have observed coherent tunneling rates that are approximately an order of magnitude higher than the phase breaking rate, thus demonstrating favorable properties of quantum antidot devices for coherent coupling of 0D states.

The quantum antidot devices were fabricated by electron beam lithography on a high mobility ($\mu \sim 2 \times 10^6$ cm^2/V s) GaAs/AlGaAs heterostructure. The inset to Fig. 1 presents an atomic force micrograph of a sample device, showing the metalization on the surface of the wafer consisting of two front gates and a small island between them. The two-dimensional electron system (2DES) is depleted under all the metalization, therefore creating a constriction with a hole in the middle (antidot). In the quantum Hall regime gapless edge channels form around the front gates, and the states circulating the antidot (area S_m) are quantized by the Aharonov-Bohm (AB) condition $BS_m = m\phi_0$, where ϕ_0 is the flux quantum and m is an integer [12]. By adjusting the gate voltages the two edges can be brought close enough to the antidot for resonant tunneling to occur. The experiments were performed at dilution refrigerator base temperature $T_{\mathrm{bath}} = 13$ mK using excitation current 50 pA, with sample electron temperature $T \approx 18$ mK, as determined from a Joule heating model [13]. Since

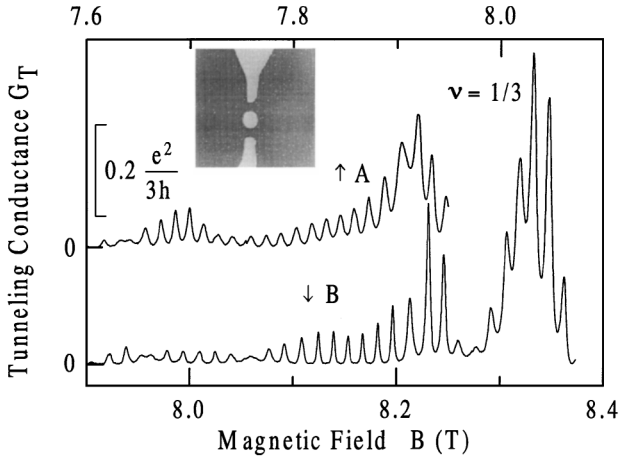

FIG. 1. Tunneling conductance as a function of magnetic field at $\nu = 1/3$. Traces A and B are from different cooldowns of the same sample. Inset: Atomic force micrograph (5 μm $\times$ 5 μm) of a representative antidot device; the experimental device has smaller lithographic antidot diameter of 200 nm. Light areas define the front gates and the antidot.

 0031-9007/00/84(8)/1776(4)$15.00

$k_BT \ll \Delta E \approx 20\ \mu$eV, the energy spacing between the antidot states [14] at the chemical potential μ, tunneling takes place through a single 0D antidot state. By changing B the antidot states will move in energy with respect to μ, thus resonances in tunneling conductance, G_T, can be observed as a function of B.

Figure 1 shows representative G_T vs B data. The two datasets A and B were measured on the same sample, but on different cooldowns. We clearly observe quasiperiodic resonant tunneling peaks, with the period ΔB giving a radius $r_m = \sqrt{\phi_0/\pi\Delta B} \approx 300$ nm for the antidot states, consistent with lithography. In addition, a striking and strong modulation of the resonance peak heights over an order of magnitude can be seen, accompanied by a 20% modulation of the widths of the resonances. As we have reported earlier [13], the resonance line shapes are dominated by thermal broadening. Within the model of a single antidot, we would then expect only a monotonic increase of the peak heights as a function of B (because of the inward movement of the edge channels) and no modulation in widths. On the other hand, tunneling via *two* antidots in series explains the experimental observations, and interesting quantitative details of the resonant states can be determined, as we demonstrate below.

A schematic diagram of the tunneling process is shown in Fig. 2(a). In addition to the series of 0D states localized on the lithographic antidot (energies ϵ_2^k), we argue there is another "impurity antidot" (with 0D states ϵ_1^j) formed by the disorder potential, located between the left edge and the lithographic antidot. This impurity antidot is smaller than the lithographic antidot, and is much closer to the left edge channel and the lithographic antidot than the latter is to the right edge channel. Therefore tunneling rates between the left edge and the impurity antidot, Γ_1, and between the impurity antidot and the lithographic antidot, Γ_{12}, are orders of magnitude higher than the tunneling rate to the right edge, Γ_2. From the quasiperiodicity of the envelope of the tunneling peaks, Fig. 1, we can estimate the area of the AB-quantized impurity antidot, corresponding to a radius $r_A \approx 80$ nm in dataset A, and $r_B \approx 100$ nm in dataset B. Converting to the energy scale [14] we get the energy spacing at μ of the impurity antidot states $\epsilon_1^j - \epsilon_1^{j+1} \approx 0.3$ meV and 0.2 meV in datasets A and B, respectively.

We use a Breit-Wigner formula to model the tunneling conductance through two sets of 0D states ϵ_1^j and ϵ_2^k in the fully coherent regime [15]. It is given by

$$G_T = \sum_{jk} \frac{e^2}{3h} \times \frac{4\Gamma_1\Gamma_{12}^2\Gamma_2}{|(\mu - \epsilon_1^j + i\Gamma_1)(\mu - \epsilon_2^k + i\Gamma_2) - \Gamma_{12}^2|^2}, \quad (1)$$

where Γ_1, Γ_2, and Γ_{12} are the tunneling rates, as shown in Fig. 2(a), and the factor of 3 accounts for the peak

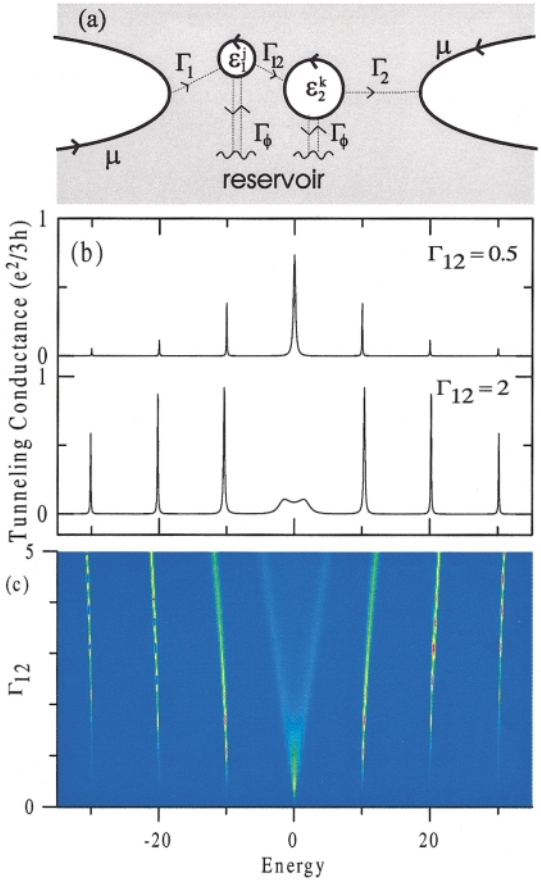

FIG. 2 (color). (a) Schematic diagram of the sample, with two antidots in series. Solid lines represent edge states, dotted lines with arrows are tunneling paths. The energy spectrum at μ is continuous in the outside edges, the antidot states are quantized and have energies ϵ_1^j and ϵ_2^k. Γs are the tunneling rates, phase breaking events have rate Γ_ϕ. (b) Theoretical coherent tunneling conductance [Eq. (1)] as a function of energy μ for two antidots in series. $\epsilon_1 = 0$, $\epsilon_2 = 10k$, where $k = 0, \pm1, \pm2, \ldots$, $\Gamma_1 = 2$, and $\Gamma_2 = 0.04$. Upper plot has $\Gamma_{12} = 0.5$, lower $\Gamma_{12} = 2$. (c) Density plot of the tunneling conductance as a function of Γ_{12}, all parameters are the same as in (b). Lighter shades correspond to higher G_T.

quasiparticle conductance at $\nu = 1/3$. Equation (1) is derived in the limit $k_BT \ll \Gamma_1, \Gamma_2, \Gamma_{12}$; below we discuss how G_T is modified at higher temperatures.

In Fig. 2(b) we plot representative theoretical G_T traces, using Eq. (1), as a function of energy μ (variation of μ corresponds to variation of B in experiment). We have set the theoretical energy units so that the energy spacing of the antidot states $\epsilon_2^k - \epsilon_2^{k+1} = 10$, and show the resulting conductance peaks around one "impurity state" at $\epsilon_1 = 0$. The tunneling rates used in Fig. 2(b) are in a realistic regime for the experiment, as estimated from the sample geometry [16]. Clearly Eq. (1) reproduces the strong modulation of the peak heights together with modulation of the widths, as seen in experiment. The modulation of conductance occurs because the states ϵ_2^k see the density of states on the left that is not constant, but modulated by the resonant levels ϵ_1^j. Whether the G_T peak at

$\mu = \epsilon_1^j$, for example $\mu = 0$ in Fig. 2(b), is the strongest or not depends very sensitively on the tunneling rates. The upper plot with $\Gamma_{12} = 0.5$ has the central peak at $\mu = 0$ the strongest, but it splits into a doublet for $\Gamma_{12} = 2$, with much lower peak height, as seen in the lower panel. This splitting is due to the strong coupling of the states bound on the two antidots, ϵ_1 and ϵ_2, reminiscent of splitting into the symmetric and antisymmetric hybridized states in diatomic molecules.

Figure 2(c) shows the effect of Γ_{12} on G_T in a density plot. Notably, it affects the conductance not only by changing the amplitudes, but by shifting the positions of the peak maxima and by destroying the exact periodicity. This is because of the formation of the hybridized states, as mentioned above. The hybridization occurs when $\Gamma_{12} > \sqrt{(\Gamma_1^2 + \Gamma_2^2)/2}$, and, in this regime the doublet splitting $\Delta \approx 2\Gamma_{12}$, as seen in Fig. 2(c). It is also important to realize that, with the exception of the central peak at $\mu = 0$, the fast rates Γ_1 and Γ_{12} have only a minor effect on the line widths, which are determined by the slow rate Γ_2.

Doublets are indeed observable in both datasets (Fig. 3), giving strong evidence for a large coherent coupling between the two antidots. Consistent with the theoretical analysis, these doublets have lower peak heights and larger widths than the adjacent peaks. Experimentally, the doublet splitting $\Delta \approx 16$ μeV, giving $\Gamma_{12} \approx 8$ μeV [17]. Moreover, the experimental energy spacings ΔE show a 20% rise around the peaks where the impurity and lithographic antidot states align (doublets or extra wide and shallow peaks), as expected from the results of modeling shown in Fig. 2(c).

At this point the effect of phase breaking scattering events should be addressed. It is known from many other tunneling systems (e.g., resonant tunneling diodes) that most experiments are in the regime of sequential resonant tunneling [18], where the particles lose their phase memory before tunneling is completed. The transition from a fully coherent regime to a sequential regime has been discussed in the literature [19,20], and, as was shown in Ref. [20], the results can be derived from Landauer-Büttiker formalism, where the phase randomizing agent (phonons, etc.) is modeled as a perfect reservoir with elastic transition rates to other reservoirs given by Γ_ϕ, the phase breaking rate. This modeling is incorporated into our "antidot molecule" system, as shown in Fig. 2(a). In Fig. 4(a) thus calculated G_T is plotted as a function of μ and Γ_ϕ. As is the case for a single antidot, the main effect of phase breaking events is to lower the peak heights and broaden their widths.

The theoretical line shapes are closely approximated by Lorentzians, although in the experiment the thermal broadening of the tunneling peak line shapes dominates [13] even at the lowest electron temperature of 18 mK. When $k_B T > \Gamma_\phi$ the theoretical Fermi-liquid line shape is a convolution of the intrinsic Lorentzian line shapes $R(\epsilon)$ broadened by Γ_ϕ (Γ_ϕ may change with T), with the Fermi-Dirac (FD) factor at a finite T:

$$G_T(\mu; \epsilon_1, \epsilon_2, \Gamma_\phi) = \int_{-\infty}^{\infty} d\epsilon R(\epsilon; \epsilon_1, \epsilon_2, \Gamma_\phi) \times \cosh^{-2}\left(\frac{\epsilon - \mu}{2k_B T}\right), \qquad (2)$$

where a semicolon separates the independent variable from the parameters. We recover the intrinsic line shapes $R(\epsilon)$ by numerically deconvoluting the measured

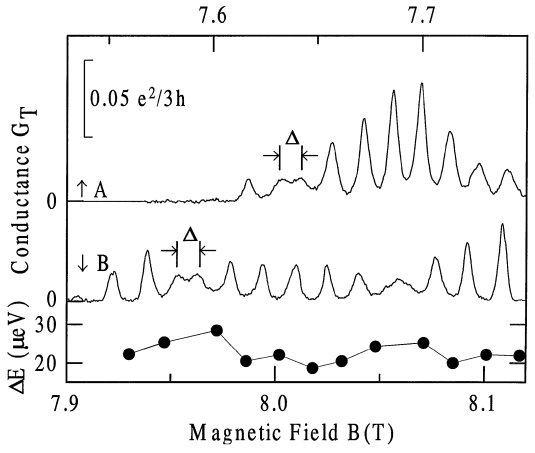

FIG. 3. Detailed plot of experimental tunneling conductance G_T, datasets A and B, showing clear doublets, together with the energy spacings ΔE of the peaks of dataset B. Near the doublet ΔE is the distance from the center of the doublet to the adjacent peaks.

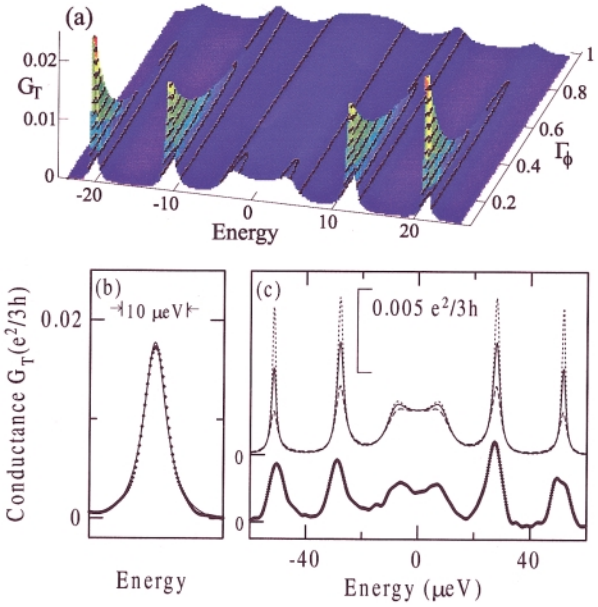

FIG. 4 (color). (a) Theoretical tunneling conductance $G_T(\mu)$ as a function of the phase breaking rate Γ_ϕ, $\Gamma_{12} = 4$. (b) The narrowest deconvoluted experimental peak (points), with a two-parameter best fit to a Lorentzian (solid line), $G_T = A/[(\epsilon - \epsilon_0)^2 + \Gamma^2]$, $\Gamma = 4$ μeV. (c) Experimental deconvoluted doublet (thick solid line) compared to numerical modeling. Solid line has $\Gamma_\phi = 0.6$ μeV, dotted line $\Gamma_\phi = 0.4$ μeV, and dashed line $\Gamma_\phi = 1$ μeV. All three have $\Gamma_1 = 6$ μeV, $\Gamma_{12} = 8$ μeV, and $\Gamma_2 = 0.005$ μeV.

tunneling peaks in energy space with the known FD factor. The narrowest deconvoluted experimental peak with a two-parameter Lorentzian fit is shown in Fig. 4(b). The fit is very good, showing that the intrinsic line shapes can indeed be resolved in our experiment. In addition, since Γ_ϕ broadens all the peaks [Fig. 4(a)], from the width of the peak shown in Fig. 4(b) we get an upper bound $\Gamma_\phi < 4\ \mu$eV. Even better, by comparing the modeling of the Γ_ϕ broadening of the doublets to the deconvoluted experimental data, Fig. 4(c), we get a best estimate $\Gamma_\phi \approx 0.6\ \mu$eV, at $T = 18$ mK. $\Gamma_\phi = 0.6\ \mu$eV corresponds to a coherence time $\tau_\phi = \hbar/\Gamma_\phi \approx 1$ ns and a coherence length $L_\phi = v_d \tau_\phi \approx 30\ \mu$m, where $v_d = 3 \times 10^4$ m/s is the drift velocity of the antidot edge states [14].

In conclusion, we have demonstrated evidence for coherent tunneling between two zero-dimensional antidot-bound states. Benefiting from the properties of the FQH condensate we can easily tune the samples to the regime where the coherent coupling between the two antidots is an order of magnitude larger than the coupling to the dephasing environment. From the numerical modeling a lower bound for the experimental dephasing time $\tau_\phi > 0.2$ ns was obtained; a more careful analysis shows that $\tau_\phi \approx 1$ ns is the best estimate. This value is of the same order of magnitude as the estimate from the coupled quantum dot experiments [7]. It should be noted that the largest lateral dimension of our sample is about 3 times larger than the one in Ref. [7], therefore by reducing the size of the antidot it may be possible to reduce phonon coupling further and thus to push τ_ϕ higher.

We would like to thank D. V. Averin and I. L. Aleiner for discussions. This work was supported in part by the N.S.F. under Grant No. DMR-9629851.

*Present address: Department of Physics and Astronomy, Michigan State University, East Lansing, MI 48824-1116.

[1] B. Su, V. J. Goldman, and J. E. Cunningham, Science **255**, 313 (1992); Phys. Rev. B **46**, 7644 (1992).
[2] Reviewed in U. Meirav and E. B. Foxman, Semicond. Sci. Technol. **10**, 255 (1995); L. P. Kouwenhoven *et al.*, in *Advanced Study Institute on Mesoscopic Electron Transport* (Kluwer Academic, MA, 1997), Series E.
[3] C. Livermore *et al.*, Science **274**, 1332 (1996).
[4] R. P. Feynman, Int. J. Theor. Phys. **21**, 467 (1982); D. Deutsch, Proc. R. Soc. (London) A **400**, 97 (1985).
[5] P. W. Shor, SIAM J. Comp. **26**, 1484 (1997).
[6] D. Loss and D. P. DiVincenzo, Phys. Rev. A **57**, 120 (1998); G. Burkard, D. Loss, and D. P. DiVincenzo, Phys. Rev. B **59**, 2070 (1999).
[7] T. H. Oosterkamp *et al.*, Nature (London) **395**, 873 (1998).
[8] In the vertical geometry, it is easier to couple two quantum dots strongly; see, e.g., T. Schmidt *et al.*, Phys. Rev. Lett. **78**, 1544 (1997). The problem with vertical devices is that they cannot be integrated into a coherent 2D array.
[9] Y. Imry, *Introduction to Mesoscopic Physics* (Oxford, New York, 1997).
[10] V. J. Goldman and B. Su, Science **267**, 1010 (1995); V. J. Goldman, Physica (Amsterdam) **1E**, 15 (1997).
[11] R. B. Laughlin, Phys. Rev. Lett. **50**, 1395 (1983).
[12] Quantization remains the same even in FQH regime; see Ref. [10].
[13] I. J. Maasilta and V. J. Goldman, Phys. Rev. B **55**, 4081 (1997).
[14] I. J. Maasilta and V. J. Goldman, Phys. Rev. B **57**, R4273 (1998).
[15] See, e.g., A. I. Larkin and K. A. Matveev, Sov. Phys. JETP **66**, 580 (1987).
[16] I. J. Maasilta, Ph.D. thesis, SUNY, Stony Brook, NY, 1998.
[17] More precisely, $\Delta = \sqrt{4\Gamma_{12}^2 + (\Delta\epsilon_0)^2}$, where $\Delta\epsilon_0$ is the bare energy separation of the two states. Here, we can exclude the possibility of an appreciable $\Delta\epsilon_0$, which would cause the doublet to become nonsymmetrical (differing peak heights).
[18] S. Luryi, Appl. Phys. Lett. **47**, 490 (1985).
[19] A. D. Stone and P. A. Lee, Phys. Rev. Lett. **54**, 1196 (1985).
[20] M. Büttiker, Phys. Rev. B **33**, 3020 (1986); IBM J. Res. Dev. **32**, 63 (1988).